Available online at www.sciencedirect.com
ScienceDirect
Neuroscience Research 58 (2007) 219–225
Neuroscience Research
www.elsevier.com/locate/neures

Update article

Watching neuronal circuit dynamics through functional multineuron calcium imaging (fMCI)

Naoya Takahashi [a], Takuya Sasaki [a], Atsushi Usami [a], Norio Matsuki [a], Yuji Ikegaya [a,b,*]

[a] *Laboratory of Chemical Pharmacology, Graduate School of Pharmaceutical Sciences, The University of Tokyo, Tokyo 113-0033, Japan*
[b] *Precursory Research for Embryonic Science and Technology (PRESTO), Japan Science and Technology Agency, 4-1-8 Honcho, Kawaguchi 332-0012, Japan*

Received 10 January 2007; accepted 5 March 2007
Available online 13 March 2007

Abstract

Functional multineuron calcium imaging (fMCI) is a large-scale optical recording technique that monitors the spatiotemporal pattern of action potentials, all at once, from large neuron populations. fMCI has unique advantages, including: (i) simultaneous recording from >1000 neurons in a wide area, (ii) single-cell resolution, (iii) identifiable location of neurons and (iv) detection of non-active neurons during the observation period. We review herein the principle, history, utility and limitations of fMCI.

Keywords: Large-scale recording; Visualization; Spike train; Neuron; Action potential; Neural network; Microcircuit; Raster plot; Complex systems

1. What is fMCI?

Brain function depends on a vast and complex network in which diverse types of neurons are interconnected. A number of studies have been conducted on the function of neuronal networks and neuronal ensembles, but the mechanisms underlying their system dynamics are poorly defined. One of the main reasons is a lack of strategies to address them appropriately.

Our current understanding of information processing by neuronal networks has relied on compiling population statistics across different recording sessions, i.e. inferring from pieces of evidence that are obtained by physiological and anatomical analysis of individual neurons and synapses or otherwise by bulk recording of averaged neuronal responses. In complex systems, however, individual units function together, exhibiting collective dynamics beyond linear expectations. Their integrative behavior cannot be explained by simply putting together the properties of individual units. Studies on network behaviors, therefore, require large-scale methods to simultaneously record from a population of individual neurons.

Over the past decade, large-scale imaging techniques have rapidly developed, including functional magnetic resonance imaging, positron-emission tomography, intrinsic optical signal imaging and voltage-sensitive dye imaging. These methods are extensively used in studying different aspects of brain function, leading to discovery of many important regimes of neural information processing. Yet, one of the significant shortcomings of these techniques is their poor spatial resolution. They cannot capture network dynamics at the single-cell level.

An alternative method is functional multineuron calcium imaging (fMCI), which can record from neuron populations with single-cell resolution. In other words, fMCI can reconstruct when, where and how individual neurons are activated in a network of interest, although its strategy is somewhat invasive to living biosystems. For fMCI, brain tissue is bulk-loaded with calcium-sensitive fluorescence indicator (Fig. 1A), and the changes in fluorescence intensity are measured from the cell bodies of neurons (Fig. 1B and C). Unlike voltage-sensitive dyes, which usually undergo a small (<1%) change in fluorescence or photoabsorption during activity, commonly used calcium indicators show 2–30% fluorescence changes in response to single action potentials (Smetters et al., 1999). The fluorescence transients arise from

* Corresponding author at: Laboratory of Chemical Pharmacology, Graduate School of Pharmaceutical Sciences, The University of Tokyo, Tokyo 113-0033, Japan. Tel.: +81 3 5841 4783; fax: +81 3 5841 4786.
E-mail address: ikegaya@mol.f.u-tokyo.ac.jp (Y. Ikegaya).

0168-0102/$ – see front matter
doi:10.1016/j.neures.2007.03.001

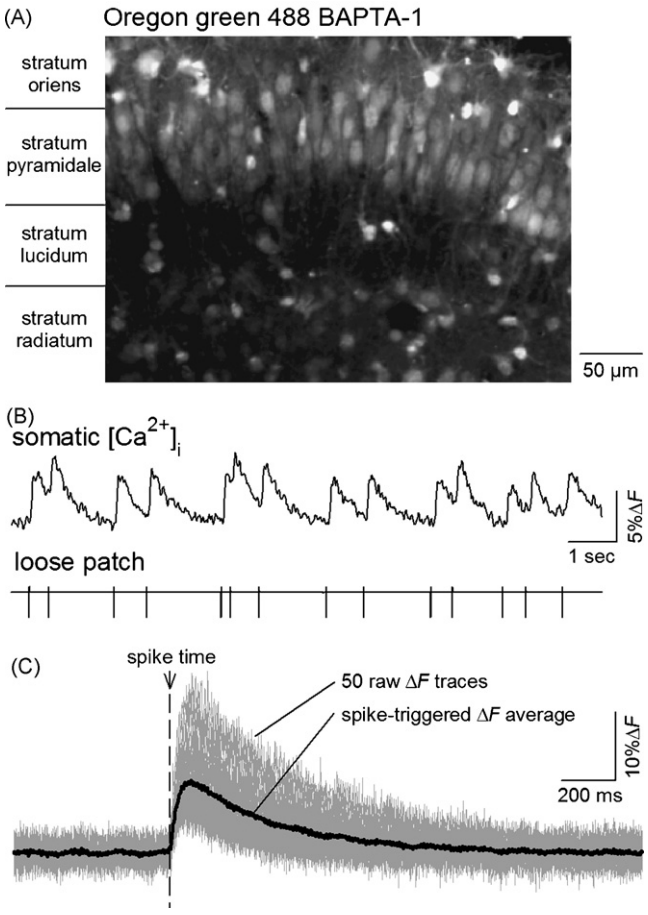

Fig. 1. fMCI detects action potentials from individual neurons. (A) Confocal image of the CA3 region in an organotypically cultured rat entorhino-hippocampal slice bolus-loaded with Oregon green 488 BAPTA-1. (B) Simultaneous monitoring of somatic calcium signal and loose-patch recording from the same neuron. Note that action potentials are mirrored in calcium transients. (C) Single spike-evoked calcium transients. Gray lines indicate merged 50 calcium traces recorded from different neurons, on which the averaged trace is superimposed as thick black line.

calcium influx through one or more types of voltage-sensitive calcium channels, and thereafter the signal may be amplified by calcium release from intracellular stores. fMCI is based on the idea that if such spike-evoked calcium transients are simultaneously imaged from numerous neurons, they would serve as large-scale dataset of active neuronal networks.

Multielectrode unit recording is another approach to examine network dynamics with single-cell resolution. At present, this method allows simultaneous recording from dozens of neurons with fine temporal resolution. But algorithms and methods for detecting and classifying action potentials from multielectrode signals, the so-called spike-sorting problem, are far from perfect at present and will become increasingly difficult with an increasing number of neurons recorded. Moreover, those data convey little information on location and type of neurons responsible for the sorted spikes. In this respect, fMCI can clearly determine the physical position of spiking neurons. Even non-active neurons can be identified during the recording period. They are not negligible, because ‘‘silence’’ also constitutes an important part of neural information. Taken together, fMCI provides a unique opportunity to reveal the morphology and function of neuronal networks.

2. Principle and history of fMCI

The synthesis of acetoxymethyl (AM) ester derivatives of calcium indicators was momentous in the history of calcium imaging (Tsien, 1981, 1988). The original form of most calcium indicators is negatively charged and does not penetrate into lipid bilayer. To enhance the membrane permeability, the charged functional groups are masked with AM ester, which makes the dyes more lipophilic. Once inside the cell, the indicator is hydrolyzed by cytoplasmic esterase and converted back to the original, negatively charged form. Thus, it accumulates inside the cell at higher concentrations than the extracellular dye concentration. In the protocol used in our laboratory (see Appendix A), the intracellular concentration of dye is estimated to reach a few tens of μM within 60 min of incubation with 4 μM of extracellular AM-ester dye solution (Sasaki et al., 2007b). Consequently, a large number of cells in brain tissue are heavily loaded with calcium indicator (Fig. 1A).

The original idea of fMCI was introduced by Yuste and Katz (1991). They used fura-2AM to image the activity of dozens of neurons in immature neocortical slices and assessed postsynaptic $[Ca^{2+}]_i$ changes elicited by excitatory and inhibitory neurotransmitters. Throughout this report, the authors emphasized the utility of fMCI to understand the network function, whereas they noted several drawbacks, including the poor temporal resolution (less than 1 Hz) and age-dependent dye-loading efficacy; samples were limited to slices prepared from neonatal or juvenile animals.

Recent improvements in optical and experimental techniques have alleviated these problems. A double incubation protocol was proposed as a means of loading into more mature brain slices. In conventional bulk-loading with fura-2AM, for example, preparations are incubated for 30–60 min with 10 μM dye solution supplemented with detergent such as Pluronic F-127 or Cremophor EL. In contrast, the double loading protocol consists of two steps: (1) an initial incubation for 1–2 min with a few drops of 1 mM dye in 100% dimethyl sulfoxide (DMSO) and then (2) a second incubation in oxygenated 10 μM dye for 30 min (Schwartz et al., 1998). This protocol made it possible to label neurons in slices prepared from rodents aged 10–30 days; the percentage of loaded cells is reported to range from 60% to 100% (Peterlin et al., 2000). At present, further improvements of slice preparations and dye incubation protocols have allowed constantly labeling ~90% of neurons in neocortical and hippocampal slices, even with a single incubation protocol with fura-2AM, fluo-4AM and Oregon green 488 BAPTA-1AM (Cossart et al., 2003; Ikegaya et al., 2004, 2005, see also Appendix A). Another strategy could be electroporation through dye-loaded glass pipettes, which allows selective labeling of a small group of neurons in a local circuit (Nagayama et al., 2007; Nevian and Helmchen, 2007).

Several research groups have developed green fluorescent protein (GFP)-based calcium probes. Some probes are

strategically designed to use a partial sequence of calcium-dependent proteins as a calcium-sensitive linker, so as to exhibit calcium-dependent changes in the efficacy of fluorescence resonance energy transfer (FRET) between two GFP variants with differing spectra (Miyawaki et al., 1997). Others use calcium-sensitive sequences inserted into specific regions of a single GFP fluorophore (Baird et al., 1999; Nagai et al., 2001; Nakai et al., 2001). Because these probes are genetically encoded, fMCI is carried out for genetically defined subpopulations of neurons without bulk dye loading. For example, Wang et al. (2003) expressed G-CaMP, a high-affinity calcium probe (Nakai et al., 2001), in primary olfactory sensory neurons and projection neurons of *Drosophila* and mapped odor-evoked activity in the antennal lobe. Transgenic mice that express genetically encoded calcium indicators are recently being used as well (Hasan et al., 2004; Pologruto et al., 2004; Díez-García et al., 2005).

3. Cell identification in fMCI

Although in our experience, fura-2AM seems to label neurons in a relatively specific manner, most calcium indicators are non-specifically loaded into cells. fMCI data, therefore, risks contamination with non-neuronal signal.

There are several ways to discriminate neurons from other types of cells. The most rigid inspection is post hoc immunostaining against neuronal markers such as neuron-specific nuclear protein (NeuN) and neuron-specific enolase (NSE) (Sasaki et al., 2007a). It also allows identification of types of neurons, e.g. calcium/calmodulin-dependent protein kinase II-positive neurons and parvalbumin-positive or cholecystokinin-positive interneurons. A shortcoming of the post hoc immunostaining is, however, that microscopic search of immunolabeled images with the same x–y field and the same z-focus plane as the fMCI movies is laborious in some cases. As a more convenient way, counterstaining with cell type-specific vital dye is available. For example, sulforhodamine 101 works as a marker for astrocytes in living tissues (Nimmerjahn et al., 2004). This dye emits red fluorescence, and hence it can be combined with green fluorescent calcium indicator.Genetically encoded fluorescent markers are also useful for cell type identification. Yaksi and Friedrich (2006) imaged odor-evoked activity of mitral cells in the zebrafish olfactory bulb. In their experiments, mitral cells were identified by colocalization of the calcium signal of rhod-2, a red fluorescent indicator, with yellow fluorescent protein that was transgenically expressed under the control of a mitral cell-specific promoter. Aguado et al. (2002) identified astrocytes in fura-2-loaded slices prepared from transgenic mice that expressed GFP with the promoter of glial fibrillary acidic protein. Sohya et al. (2007) identified inhibitory interneurons in fura-2-loaded tissues of transgenic mice, in which GABAergic neurons express enhanced GFP.

We would like to emphasize, however, that cell morphology and calcium transient kinetics alone are enough to distinguish between neurons and non-neuronal cells. In fluorescence images of slices stained with Oregon green 488 BAPTA-1AM or fluo-4AM, non-neuronal cells have smaller somata and higher baseline brightness than neurons. Therefore, we can identify neurons with approximately 97% confidence (i.e. error detection = ∼3%) without specific cell markers (Sasaki et al., 2007a). In addition, glial calcium waves usually exhibit much slower kinetics and higher amplitude, as compared to spike-triggered neuronal calcium transients (Ikegaya et al., 2005). Thus, if cells that displayed slow Ca^{2+} transients with a more than 200 ms peak latency are discarded, the remaining data are only minimally contaminated with non-neuronal signals.

4. Temporal resolution of fMCI

Poor temporal resolution is a major limitation of fMCI; typical frame rates are 0.5–30 Hz. Such slow time-lapse imaging lacks the temporal precision to investigate features of neuronal spike activity such as synchronization or oscillation. To overcome this disadvantage, Mao et al. (2001) used a photodiode array with 464 detectors to attain high-speed recording (450–1666 Hz). They recorded spontaneous activity of neuron populations in slices of mouse primary visual cortex and found that precisely timed synchronization and sequential activation among neurons occurred more frequently than expected by chance. In this approach, however, neuronal activity was recorded only as a one-dimensional fluorescence trace (not two-dimensional planar images), and information on cell morphology was not available. Moreover, the number of neurons recorded is limited to the number of detectors in the photodiode array.

We have recently used a high-speed charge-coupled device camera and a fast spinning-disk confocal microscope equipped with a high-numerical-aperture low-magnitude objective (see Appendix A). We succeeded in acquiring two-dimensional images at up to 1000 Hz (Takahashi et al., 2007). This fast

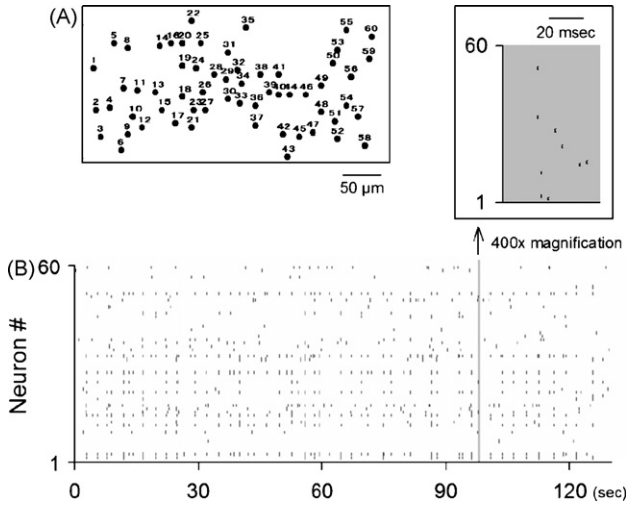

Fig. 2. High-speed fMCI reveals the millisecond structure of active network dynamics. Sixty neurons in hippocampal CA3 stratum pyramidale are imaged at 500 Hz (=every 2 ms). Data include pyramidal cells and interneurons, which are not discriminated here. (A) Positions of 60 arbitrarily numbered neurons. (B) Rastergram representing the spatiotemporal pattern of spontaneous spike activity of 60 neurons. Each row represents a single neuron, and each mark the onset of a calcium transient. The time axis of the shaded narrow area is 400 times expanded in the top-right inset so that one can see the temporal microstructure of synchronization by 9 of 60 neurons.

fMCI allows us to investigate the millisecond structure of individual neuronal activities on a large scale (Fig. 2).

Temporal resolution is also enhanced by scanning with acousto-optic deflectors (AOD), in which the direction of a light beam is controlled by the adjustable pitch of diffraction gratings that are created with a planar sound wave of radio frequency traveling through an acousto-optic medium. Unlike galvanomirror optics, etc., AOD is a non-mechanical device, so it attains high-speed scanning even from discontinuous points. Salomé et al. (2006) used two AOD devices for random-access, point-to-point recordings in two-photon microscopy and performed 100-Hz recordings of spontaneous calcium transients from cultured hippocampal neurons.

There is also a mathematical solution to enhance temporal resolution. During trains of action potentials, individual unitary calcium transients summate and generate complex temporal variations in $[Ca^{2+}]_i$. Because of slow $[Ca^{2+}]_i$ decay with a time constant of hundreds of milliseconds (cf. ~1-ms duration of action potential), individual action potentials emitted at high firing rates or burst trains may appear inseparable in calcium traces. Assuming that $[Ca^{2+}]_i$ variations are approximated by a convolution of an action potential train with the waveform of a unitary calcium transient, the temporal pattern of changes in firing rates can be deconvoluted from the time course of calcium signal. Using this temporally deconvolved fMCI, Yaksi and Friedrich (2006) reconstructed odor-evoked and spontaneous firing rate changes across neuronal populations in the olfactory bulb in adult zebrafish.

5. Spatial resolution of fMCI and in vivo imaging

The greatest advantage of fMCI is large-scale measurement with single-cell-resolution and identifiable location. The size of a neuron population recorded by fMCI is far larger than that recorded by any other optical or electrophysiological technique at present. In the neocortex, fMCI can visualize more than 1000 neurons (Cossart et al., 2003; Ikegaya et al., 2004; Ohki et al., 2005, 2006), although the maximal number of imageable neurons is relatively low in the hippocampus because of the narrow neuron packing in the pyramidal cell layer.

fMCI displays its real utility when used with multiphoton microscopy. With a local pressure injection technique through glass pipettes, Stosiek et al. (2003) delivered AM-ester dye deep inside the brain of anesthetized mice and imaged neurons up to 300 μm below the cortical surface with a two-photon microscope. They measured whisker deflection-evoked calcium transients in layer 2/3 neurons of the barrel cortex. Applying the same procedure to the primary visual cortex, Ohki et al. (2005, 2006) examined the functional architecture of orientation and direction selectivity to visual stimuli. They demonstrated the existence of sharp borders, at the level of individual neurons, in direction preference and pinwheel centers. Before these studies, such architectures could only be assessed by microelectrode recordings, which typically sampled one or a few neurons. Thus, in vivo fMCI provides a powerful tool to elucidate the relationship between cortical maps and electrophysiological dynamics of spiking neurons.

A fast three-dimensional imaging approach has recently been exploited in practical use. This approach is based on piezoelectrically induced mechanical vibration of a microscope objective (Sasaki et al., 2007b). Göbel et al. (2007) combined a continuous two-photon line-scanning procedure with sinusoidal up-down objective movement and achieved 10-Hz imaging from hundreds of neocortical neurons and astrocytes in volumes of up to 250-μm side length in anesthetized rats.

6. Synaptic connectivity revealed by fMCI

Intracellular recordings using patch-clamp and sharp electrodes can reveal the connectivity of microcircuits as well as the properties of the recorded neurons and synapses. For example, patch-clamp recordings from multiple neurons, combined with anatomical reconstruction, can reveal the properties of single synaptic transmission (Markram et al., 1997) and network connectivity (Song et al., 2005). The probability that randomly chosen neurons are monosynaptically connected, however, is low, and thus, comprehensive reconstruction of neural circuits is largely impractical. fMCI can address this problem. By searching for neurons that produce calcium transients time-locked to spikes of a given 'trigger' cell, which is electrically stimulated during fMCI, one can detect synaptically connected pairs of neurons with high success rates (Peterlin et al., 2000). Kozloski et al. (2001) utilized this optical probing technique and found that identified postsynaptic cells were stereotypically located relative to the presynaptic neurons. In contrast, a technique named reverse optical probing (ROPing) reveals presynaptically connected neurons (Aaron and Yuste, 2006). ROPing is based on an idea that a surrounding neuron that shows calcium transients immediately before postsynaptic currents occur in a given neuron is likely to form a presynaptic contact with the recorded neuron. Because monosynaptically connected neurons are rapidly detected, these optical probing techniques are useful to systematically track neuronal circuits in real time.

7. Circuit input and output assessed by fMCI

fMCI is also applicable to measuring the input and output relationship of neuronal activity in a local circuit. In the motor or somatosensory cortex of anesthetized rats, Kerr et al. (2005) compared the number of postsynaptic spikes to bulk calcium signal in the neuropil region devoid of cell bodies, which provided a measure of local synaptic input levels, i.e. the approximate number of activated presynaptic axons. They found that spontaneous fluctuations in the neuropil signal, rather than postsynaptic spikes, are correlated with local field potentials, thus termed optical encephalogram.

Hippocampal slice preparations are especially suitable to examine the input–output relationship, because the neuron-rich and neuron-poor areas are laminarly segmented. In the presence of inhibitors of fast synaptic transmission, we monitored calcium signal from CA1 stratum radiatum, where CA3 axons run, in response to extracellular stimulation of the axon bundle. We also imaged action potential-evoked calcium transients of

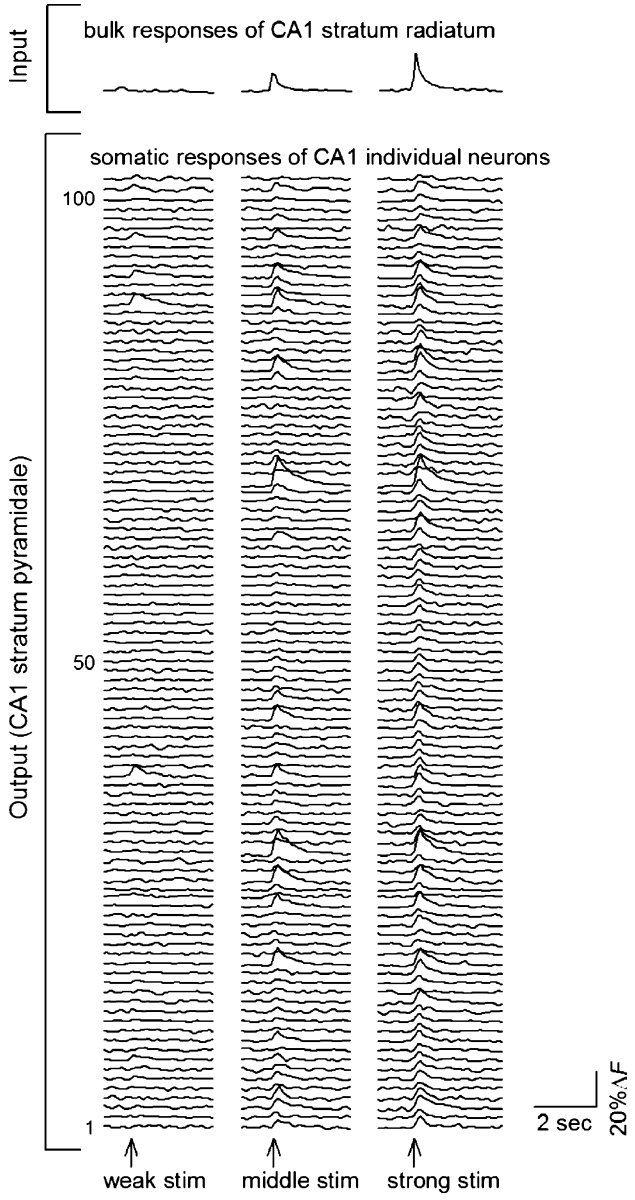

Fig. 3. fMCI can separate the microcircuit input and output. Schaffer collateral afferents were stimulated to activate CA1 neurons in a rat hippocampal slice. Input was monitored as a bulk response recorded from CA1 stratum radiatum in the presence of synaptic inhibitor cocktail (top), while output responses were monitored from the somata of 101 individual neurons located in CA1 stratum pyramidale (bottom). Note that input responses show a gradual increase in size as the stimulus intensity is strengthened, whereas network outputs are obtained as individual all-or-none responses.

individual CA1 neurons in the pyramidal cell layer (Fig. 3). This experiment is designed to examine the input–output relationship of a CA1 local circuit. We found that the CA1 network responds linearly to single-pulse input, but non-linearly to multi-pulse inputs (Sasaki et al., 2006).

8. Automated fMCI

For practical use of fMCI, we have developed an efficient algorithm that automatically extracts the onset times of action potential-evoked calcium transients from raw fluorescent traces. In previous studies, reconstruction of neuronal activity has mostly relied on a manual, offline process, which requires time and effort and is accompanied by a risk of artificial errors, because the size of fMCI data is inevitably huge. Our spike-detection algorithm employs principal component analysis and support vector machines. Specifically, the wave form of calcium signal is normalized for amplitude, compressed through principal component analysis, and then surveyed by linear support vector machine to classify each wave segment into an event with or without an action potential (Sasaki et al., 2007b). Because this process is mathematically simple, the computation is fast enough to be used online. At present, the accuracy of spike detection reaches 93% on average, which is more precise than the human eye (about 80%).

9. Future perspectives on fMCI

Large-scale recordings from neuron populations are indispensable for the understanding of neuronal circuit operations. As one such approach, we reviewed here the utility and recent improvements of fMCI. As repeatedly described above, fMCI is technically a powerful tool, but now, a major problem confronting fMCI is a lack of mathematical or computational supports for large-scale analysis of fMCI data. The theoretical backbone for data-mining from multineuronal spike trains is still rudimental. There is obviously a need for fruitful collaborations of experimentalists and theorists. As a first step, we have opened our fMCI data to the public so that anyone can freely download and analyze them (http://hippocampus.jp/data/). We believe that such open-access data archives and information sharing platforms facilitate research on neuronal network dynamics.

The collective dynamics of neurons such as synchronization and oscillation, are not only involved in cognitive or motorsensory processing in the normal brain, but they also contribute to pathogenesis in disorders, including epilepsy, schizophrenia, autism, multiple sclerosis, and Alzheimer's and Parkinson's diseases (Uhlhaas and Singer, 2006). fMCI may offer a new-generation experimental platform for detecting functional abnormalities of neuronal networks and screening novel lead compounds of therapeutic drugs.

Acknowledgements

This work was supported in part by a Grant-in-Aid for Science Research on Priority Areas (Elucidation of neural network function in the brain: No. 18021008); a Grant-in-Aid for Science Research (Nos. 17650090 and 17689004) from the Ministry of Education, Culture, Sports, Science and Technology of Japan; KONICA MINOLTA Imaging Science Foundation; and the Narishige Neuroscience Research Foundation. We are grateful to Dr. Wolfram Schleich and Neil Gray for giving their comments on this manuscript.

Appendix A

Lab protocol for bulk loading of Oregon green 488 BAPTA-1AM

A.1. Reagents

Oregon green 488 BAPTA-1AM: Invitrogen O-6807, 50 μg × 10, special packaging.
Cremophor EL: Sigma–Aldrich C-5135, 100 g.
Pluronic F-127: Invitrogen P-6867, 2 g.
(±)*Sulfinpyrazone*: Sigma–Aldrich S9509, 5 g.

A.2. Stock solutions

(i) *0.1% Oregon green BAPTA-1AM*: Add 50 μl DMSO to a 50-μg package tube. Dispense each 10 μl solution to a 1.5 ml tube and store in a −20 °C freezer. Other Ca^{2+} indicators such as fura-2AM and fluo-4AM, can be prepared in the same procedure.
(ii) *5% Cremophor EL*: Dilute 0.5 ml Cremophor EL in 9.5 ml DMSO in a 15 ml tube. Careful measuring is required because Cremophor EL is a viscoelastic liquid. Store the solution at room temperature.
(iii) *10% Pluronic F-127*: Dissolve 100 mg Pluronic F-127 in 1 ml DMSO in a 1.5 ml tube. Store at room temperature. Do not use a stock that contains any crystallized material after long-term storage.
(iv) *100 mM* (±)*sulfinpyrazone*: Dissolve 40 mg (±)sulfinpyr-sulfinpyrazone in 1 ml DMSO in a 1.5 ml tube. Store at room temperature.

A.3. Preparations

(v) *Brain slices*: Prepare acute slices (350–500 μm of thickness) from immature or young animals. Rodents aged less than 16 days are desirable. Organotypic slice cultures are also usable, generally giving better dye loading than acute slices.
(vi) *Artificial cerebrospinal fluid* (*aCSF*): aCSF consists of (in mM): 127 NaCl, 26 $NaHCO_3$, 1.5 KCl, 1.24 KH_2PO_4, 1.4 $MgSO_4$, 2.4 $CaCl_2$ and 10 glucose. Bubble aCSF with 95% O_2 and 5% CO_2 throughout experiment.
(vii) *Dye solution*: Add 10 μl of solution (i) and each 2 μl of solution (ii), (iii) and (iv) to 2 ml aCSF (vi) in a 50 ml tube. Sonicate this mixture with an ultrasonicator with a microtip (1-s duration, 50 times at an interval of 1 s). The final solution contains 0.0005% (∼4 μM) Oregon green 488 BAPTA-1AM, 0.005% Cremophor EL, 0.01% Pluronic F-127, 100 μM (±)sulfinpyrazone and 0.775% DMSO.

A.4. Loading method

(1) Submerge brain slices into the dye solution (vii) in a 35 mm dish.
(2) Incubate them at 37 °C for 45–60 min, during which 95% O_2 and 5% CO_2 are continuously supplied under moist conditions. Care must be taken to avoid drying due to bubbling. For organotypic slice cultures, put the dish in a cell-culture CO_2 incubator at 37 °C for 60 min.
(3) Terminate the incubation by transferring the slices into fresh aCSF (vi) and leave them for at least 60 min before imaging.

A.5. Lab apparatus and equipment

Spinning-disk confocal system: Yokogawa Electric CSU22, preproduction CSUX and custom-remodeled CSU10.
Electron-multiplying charge-coupled device camera: Andor iXon DU860 and DV887.
Upright microscope: Nikon ECLIPSE FN1.
Water-immersion objective: Nikon CFI75 LWD 16XW, 16×, 0.80 numerical aperture.
Image-acquisition software: Andor iQ, Andor Solis, and Molecular Devices Metamorph.

References

Aaron, G., Yuste, R., 2006. Reverse optical probing (ROPing) of neocortical circuits. Synapse 60, 437–440.
Aguado, F., Espinosa-Parrilla, J.F., Carmona, M.A., Soriano, E., 2002. Neuronal activity regulates correlated network properties of spontaneous calcium transients in astrocytes in situ. J. Neurosci. 22, 9430–9444.
Baird, G.S., Zacharias, D.A., Tsien, R.Y., 1999. Circular permutation and receptor insertion within green fluorescent proteins. Proc. Natl. Acad. Sci. U.S.A. 96, 11241–11246.
Cossart, R., Aronov, D., Yuste, R., 2003. Attracter dynamics of network UP states in the neocortex. Nature 423, 283–288.
Díez-García, J., Matsushita, S., Mutoh, H., Nakai, J., Ohkura, M., Yokoyama, J., Dimitrov, D., Knöpfel, T., 2005. Activation of cerebellar parallel fibers monitored in transgenic mice expressing a fluorescent Ca^{2+} indicator protein. Eur. J. Neurosci. 22, 627–635.
Göbel, W., Kampa, B.M., Helmchen, F., 2007. Imaging cellular network dynamics in three dimensions using fast 3D laser scanning. Nat. Methods 4, 73–79.
Hasan, M.T., Friedrich, R.W., Euler, T., Larkum, M.E., Giese, G., Both, M., Duebel, J., Waters, J., Bujard, H., Griesbeck, O., Tsien, R.Y., Nagai, T., Miyawaki, A., Denk, W., 2004. Functional fluorescent Ca^{2+} indicator proteins in transgenic mice under TET control. PLoS Biol. 2, 763–775.
Ikegaya, Y., Aaron, G., Cossart, R., Aronov, D., Lampl, I., Ferster, D., Yuste, R., 2004. Synfire chains and cortical songs: temporal modules of cortical activity. Science 304, 559–564.
Ikegaya, Y., Bon-Jego, M.L., Yuste, R., 2005. Large-scale imaging of cortical network activity with calcium indicators. Neurosci. Res. 52, 132–138.
Kerr, J.N.D., Greenberg, D., Helmchen, F., 2005. Imaging input and output of neocortical networks in vivo. Proc. Natl. Acad. Sci. U.S.A. 102, 14063–14068.
Kozloski, J., Hamzei-Sichani, F., Yuste, R., 2001. Stereotyped position of local synaptic targets in neocortex. Science 293, 868–872.
Markram, H., Lübke, J., Frotscher, M., Sakmann, B., 1997. Regulation of synaptic efficacy by coincidence of postsynaptic APs and EPSPs. Science 275, 213–215.
Mao, B.Q., Hamzei-Sichani, F., Aronov, D., Froemke, R.C., Yuste, R., 2001. Dynamics of spontaneous activity in neocortical slices. Neuron 32, 883–898.
Miyawaki, A., Llopis, J., Heim, R., McCaffery, J.M., Adams, J.A., Ikura, M., Tsien, R.Y., 1997. Fluorescent indicators for Ca^{2+} based on green fluorescent proteins and calmodulin. Nature 388, 882–887.
Nagai, T., Sawano, A., Park, E.S., Miyawaki, A., 2001. Circularly permuted green fluorescent proteins engineered to sense Ca^{2+}. Proc. Natl. Acad. Sci. U.S.A. 98, 3197–3202.
Nagayama, S., Zeng, S., Xiong, W., Fletcher, M.L., Masurkar, A.V., Davis, D.J., Pieribone, V.A., Chen, W.R., 2007. In vivo simultaneous tracing and Ca^{2+} imaging of local neuronal circuits. Neuron 53, 789–803.

Nakai, J., Ohkura, M., Imoto, K., 2001. A high signal-to-noise Ca^{2+} probe composed of a single green fluorescent protein. Nat. Biotechnol. 19, 137–141.

Nevian, T., Helmchen, F., 2007. Calcium indicator loading of neurons using single-cell electroporation. Pflugers Arch. in press.

Nimmerjahn, A., Kirchhoff, F., Kerr, J.N.D., Helmchen, F., 2004. Sulforhodamine 101 as a specific marker of astroglia in the neocortex in vivo. Nat. Methods 1, 1–7.

Ohki, K., Chung, S., Ch'ng, Y.H., Kara, P., Reid, R.C., 2005. Functional imaging with cellular resolution reveals precise micro-architecture in visual cortex. Nature 433, 597–603.

Ohki, K., Chung, S., Kara, P., Hübener, M., Bonhoeffer, T., Reid, R.C., 2006. Highly ordered arrangement of single neurons in orientation pinwheels. Nature 442, 925–928.

Peterlin, Z.A., Kozloski, J., Mao, B.Q., Tsiola, A., Yuste, R., 2000. Optical probing of neuronal circuits with calcium indicators. Proc. Natl. Acad. Sci. U.S.A. 97, 3619–3624.

Pologruto, T.A., Yasuda, R., Svoboda, K., 2004. Monitoring neural activity and $[Ca^{2+}]$ with genetically encoded Ca^{2+} indicators. J. Neurosci. 24, 9572–9579.

Salomé, R., Kremer, Y., Dieudonné, S., Léger, J.-F., Krichevsky, O., Wyart, C., Chatenay, D., Bourdieu, L., 2006. Ultrafast random-access scanning in two-photon microscopy using acousto-optic deflectors. J. Neurosci. Methods 154, 161–174.

Sasaki, T., Kimura, R., Tsukamoto, M., Matsuki, N., Ikegaya, Y., 2006. Integrative spike dynamics of rat CA1 neurons: a multineuronal imaging study. J. Physiol. 574, 195–208.

Sasaki, T., Matsuki, N., Ikegaya, Y., 2007a. Metastability of active CA3 networks. J. Neurosci. 27, 517–528.

Sasaki, T., Takahashi, N., Matsuki, N., Ikegaya, Y., 2007b. Fast and accurate automatic spike detection in multi-neuronal calcium imaging: implications for a new drug-screening method in systems neuropharmacology. J. Pharmacol. Sci. (Suppl.), P1-021.

Schwartz, T.H., Rabinowitz, D., Unni, V., Kumar, V.S., Smetters, D.K., Tsiola, A., Yuste, R., 1998. Networks of coactive neurons in developing layer 1. Neuron 20, 541–552.

Smetters, D., Majewska, A., Yuste, R., 1999. Detecting action potentials in neuronal populations with calcium imaging. Methods 18, 215–221.

Sohya, K., Kameyama, K., Yanagawa, Y., Obata, K., Tsumoto, T., 2007. GABAergic neurons are less selective to stimulus orientation than excitatory neurons in layer II/III of visual cortex, as revealed by in vivo functional Ca^{2+} imaging in transgenic mice. J. Neurosci. 27, 2145–2149.

Song, S., Sjöström, P.J., Reigl, M., Nelson, S., Chklovskii, D.B., 2005. Highly nonrandom features of synaptic connectivity in local cortical circuits. PLoS Biol. 3, 507–517.

Stosiek, C., Garaschuk, O., Holthoff, K., Konnerth, A., 2003. In vivo two-photon calcium imaging of neuronal networks. Proc. Natl. Acad. Sci. U.S.A. 100, 7319–7324.

Takahashi, N., Sasaki, T., Matsuki, N., Ikegaya, Y., 2007. Fast-scanning multi-neuronal calcium imaging: implications for a new drug-screening method in systems neuropharmacology. J. Pharmacol. Sci. (Suppl.), P1-023.

Tsien, R.Y., 1981. A non-disruptive technique for loading calcium buffers and indicators into cells. Nature 290, 527–528.

Tsien, R.Y., 1988. Fluorescence measurement and photochemical manipulation of cytosolic free calcium. Trends Neurosci. 11, 419–424.

Uhlhaas, P.J., Singer, W., 2006. Neural synchrony in brain disorders: relevance for cognitive dysfunctions and pathophysiology. Neuron 52, 155–168.

Wang, J.W., Wong, A.M., Flores, J., Vosshall, L.B., Axel, R., 2003. Two-photon calcium imaging reveals an odor-evoked map of activity in the fly brain. Cell 112, 271–282.

Yaksi, E., Friedrich, R.W., 2006. Reconstruction of firing rate changes across neuronal populations by temporally deconvolved Ca^{2+} imaging. Nat. Methods 3, 377–383.

Yuste, R., Katz, L.C., 1991. Control of postsynaptic Ca^{2+} influx in developing neocortex by excitatory and inhibitory neurotransmitters. Neuron 6, 333–344.